A comprehensive genome variation map of melon identifies multiple domestication events and loci influencing agronomic traits

Guangwei Zhao[1,20], Qun Lian[2,20], Zhonghua Zhang[3,4,20], Qiushi Fu[3,20], Yuhua He[1], Shuangwu Ma[1], Valentino Ruggieri[5,6], Antonio J. Monforte[7], Pingyong Wang[1], Irene Julca[8,9,10], Huaisong Wang[3], Junpu Liu[1], Yong Xu[11], Runze Wang[12], Jiabing Ji[2], Zhihong Xu[1], Weihu Kong[1], Yang Zhong[2], Jianli Shang[1], Lara Pereira[5,6], Jason Argyris[5,6], Jian Zhang[1], Carlos Mayobre[5,6], Marta Pujol[5,6], Elad Oren[13], Diandian Ou[1], Jiming Wang[1], Dexi Sun[1], Shengjie Zhao[1], Yingchun Zhu[1], Na Li[1], Nurit Katzir[13], Amit Gur[13], Catherine Dogimont[14], Hanno Schaefer[15], Wei Fan[2], Abdelhafid Bendahmane[14], Zhangjun Fei[16,17], Michel Pitrat[14], Toni Gabaldón[9,10,18], Tao Lin[2,19], Jordi Garcia-Mas[5,6]*, Yongyang Xu[1]*, Sanwen Huang[2]*

[1]Zhengzhou Fruit Research Institute, Chinese Academy of Agricultural Sciences, Zhengzhou, China.

[2]Lingnan Guangdong Laboratory of Modern Agriculture, Genome Analysis Laboratory of the Ministry of Agriculture, Agricultural Genomics Institute at Shenzhen, Chinese Academy of Agricultural Sciences, Shenzhen, China.

[3]Key Laboratory of Biology and Genetic Improvement of Horticultural Crops of the Ministry of Agriculture, Sino-Dutch Joint Laboratory of Horticultural Genomics, Institute of Vegetables and Flowers, Chinese Academy of Agricultural Sciences, Beijing, China.

[4]College of Horticulture, Qingdao Agricultural University, Qingdao, China.

[5]Centre for Research in Agricultural Genomics CSIC-IRTA-UAB-UB, Barcelona, Spain.

[6]Institut de Recerca i Tecnologia Agroalimentàries (IRTA), Barcelona, Spain.

[7]Instituto de Biologia Molecular y Celular de Plantas, Universitat Politecnica de Valencia-Consejo Superior de Investigaciones Cientificas (CSIC-UPV), Valencia, Spain.

[8]Universitat Autònoma de Barcelona (UAB), Barcelona, Spain.

[9]Centre for Genomic Regulation (CRG), Barcelona Institute of Science and Technology,

Barcelona, Spain.

[10]Universitat Pompeu Fabra (UPF), Barcelona, Spain.

[11]National Watermelon and Melon Improvement Center, Beijing Academy of Agricultural and Forestry Sciences, Key Laboratory of Biology and Genetic Improvement of Horticultural Crops (North China), Beijing Key Laboratory of Vegetable Germplasm Improvement, Beijing, China.

[12]Centre of Pear Engineering Technology Research, State Key Laboratory of Crop Genetics and Germplasm Enhancement, Nanjing Agricultural University, Nanjing, China.

[13]Plant Science Institute, Israeli Agricultural Research Organization, NeweYa‘ar Research Center, Ramat Yishay, Israel.

[14]INRA, Génétique et Amélioration des Fruits et Légumes, Montfavet, France.

[15]Department of Ecology and Ecosystem Management, Plant Biodiversity Research, Technical University of Munich, Freising, Germany.

[16]Boyce Thompson Institute for Plant Research, Cornell University, Ithaca, NY, USA.

[17]US Department of Agriculture–Agricultural Research Service, Robert W. Holley Center for Agriculture and Health, Ithaca, NY, USA.

[18]Institució Catalana de Recercai Estudis Avançats (ICREA), Pg. Lluís Companys, Barcelona, Spain.

[19]China Agricultural University, College of Horticulture, Beijing, China.

[20]These authors contributed equally to this work.

*For correspondence: Sanwen Huang, huangsanwen@caas.cn; Yongyang Xu, xuyongyang@caas.cn; Jordi Garcia-Mas, Jordi.Garcia@irta.cat.

ABSTRACT

Melon is an economically important fruit crop that has been cultivated for thousands of years; however, the genetic basis and history of its domestication still remain largely unknown. Here, we report a comprehensive melon genomic variation map derived from the resequencing of 1,175 accessions representing the global diversity of the species. Our results suggest that three independent domestication events occurred in melon, two in India and one in Africa. We detected two independent sets of domestication sweeps, resulting in diverse characteristics of the two subspecies, *melo* and *agrestis*, during melon breeding. Genome-wide association studies for 16 agronomic traits identified 208 loci significantly associated with fruit mass, quality and morphological characters. This study sheds light on the domestication history of melon and provides a valuable resource for genomics-assisted breeding in this important crop.

INTRODUCTION

Melon (*Cucumis melo* L.), an important crop in the Cucurbitaceae family, is cultivated worldwide, with more than 32 million tons produced in 2017 (United Nations Food and Agriculture Organization (FAO) statistics), and was domesticated four thousand years ago[1]. Since most wild *Cucumis* species emerged in Africa and have the same chromosome number as *C. melo*, it has been proposed that the center of origin of cultivated melon is Africa[2,3]. However, recent studies revealed that the closest wild relatives of melon are found in India and Australia[4,5]. Melon has been classified into two subspecies, *C. melo* subsp. *melo* (*melo*) and *C. melo* subsp. *agrestis* (*agrestis*), based on ovary pubescence[6]. Both domesticated subspecies exhibit increased size of fruit, leave and seed, and loss of fruit bitterness and acidity. However, the fruit sizes of the two domesticated subspecies are highly different, and bitterness was fully lost in *melo*, but partially in *agrestis*. Therefore, the history and genetic basis of melon domestication still

remain poorly understood. Current knowledge of melon domestication is largely derived from molecular marker analyses[7,8], and limited archaeological[9] and historical data[10]. The availability of the melon genome sequence (454 Mb)[11] and a collection of melon germplasm resources made it possible to rapidly detect genomic variations and to offer new and powerful insights into the trajectory of melon domestication on a genome-wide scale.

Cucumis melo is a highly diversified species and a model system for studying several important biological processes[11], but only limited number of genes related to agronomic traits like fruit monoecy[12], flesh color[13] and peel color[14] have been identified. Genome-wide association studies (GWAS) are a powerful approach for identifying genes or quantitative trait loci (QTLs) underlying complex traits as has been demonstrated in rice[15], maize[16], foxtail millet[17], soybean[18], cotton[19], cucumber[20], and tomato[21,22]. Here we present the genome resequencing of 1,175 diverse accessions to characterize the population structure and domestication history of melon, and we provide genomic evidence for elucidating melon taxonomy. We also performed GWAS to identify a number of candidate genes and loci underlying several important agricultural traits.

RESULTS

Melon genome variation map

We used 1,175 diverse accessions of *C. melo*, which included 667 from subspecies *melo* and 508 from *agrestis*, and an additional 9 from closely related species (Fig. 1a and Supplementary Table 1). The *C. melo* collection consisted of 134 wild and 1,041 cultivated accessions spanning most of the species' native range. We generated a total of 4.29 trillion base pairs of sequence using next-generation sequencing technology, with a median depth of 4.98-fold and coverage of 80.73% of the assembled melon genome[23] (released 3.5.1). After aligning the reads against the melon reference genome[23], we identified a total of

5,678,165 single-nucleotide polymorphisms (SNPs) and 957,421 small indels (≤ 5 bp), with an average of 13.99 SNPs and 2.36 indels per kilobase (Supplementary Fig. 1, Supplementary Tables 2 and 3) that is similar to cucumber (17.22 SNPs and 1.75 indels per kilobase)[24]. The accuracy of the identified SNPs was estimated to be 99.07% when comparing 10 pairs of accessions sequenced with low (4.71 ×) and high depth (18.92 ×) (Supplementary Table 4). A total of 197,113 SNPs (3.47%) and 10,114 (1.06%) indels were located in the coding regions, among which 13,022 showed potentially large effects: 7,030 SNPs (0.12%) affected 5,598 genes by causing start codon changes, premature stop codons or elongated transcripts, and 5,992 (0.63%) indels led to frame-shift in 4,587 annotated genes (Supplementary Tables 2 and 3). Collectively, this comprehensive melon genome variation dataset provides a new resource for melon biology and breeding.

Population structure

The phylogenetic relationships for these melon accessions were inferred using a subset of 17,055 SNPs at four-fold degenerate sites. To better deduce the relationships of melon accessions from different areas, 207 with uncertain origin were excluded in the next analysis. The phylogenetic tree based on the nuclear and chloroplast genome SNPs (Fig.1b and Supplementary Fig. 2) supported three distinct clades, which exhibited strong geographic separation and distinctive botanical features. We found that only the primitive African domesticated types (CAF) were clustered with wild African accessions (WAF) in Clade I (AF), suggesting the marginal impact of WAF during melon domestication outside of Africa, consistent with a previous study[5]. The remaining accessions in Clade II and Clade III corresponded to *melo* and *agrestis* subspecies according to passport information and morphological characteristics. A similar result was obtained by DAPC analysis (Supplementary Fig. 3).

Model-based clustering and principal component (PCA) analyses further classified

each of Clade II and Clade III into two main subclades (Fig. 1c and Supplementary Fig. 4). The majority of *C. melo* var. *momordica* (*momordica*) accessions native to India, and traditionally considered as cultivated *agrestis*, formed a single subclade (Clade II-1) with an obvious admixture in genetic composition (Fig. 1c), and closely clustered together with cultivated *melo* accessions (Clade II-2). In addition, Clade II-1 generally showed similar characteristics to wild melon, such as monoecy, low sugar content, acid flesh and high resistance to pests and disease[25]. Thus, our data suggested that cultivated *melo* was domesticated directly from *momordica* (Fig. 1b). Clade III-1 consisted of wild (*C. melo* L. var. *agrestis*) and cultivated *agrestis* accessions. In this clade, the cultivated *agrestis* accessions from southern Africa unexpectedly clustered with wild *agrestis* melon derived from India. These accessions share similarities to wild melon from India with respect to bearing small fruits, monoecy and having gelatinous sheath around the seeds. Based on both genetic and trait similarities, South African *agrestis* accessions could represent recent migrants from India. Both morphological and genomic data largely support that the cultivated *melo* (Clade II-2; CM) and *agrestis* (Clade III-2; CA) accessions were domesticated from Clade II-1 (wild *melo*; WM) and Clade III-1 (wild *agrestis*; WA), respectively. Finally, we can speculate that there were three independent domestication events leading to the three main clusters: two occurring in India and another in Africa, consistent with a recent study[5]. Due to the relatively few wild African melon accessions in our study and their low influence during melon domestication, we used the melon accessions from Clade II and Clade III for further analyses.

Nucleotide diversity measured by the π value[26] for the WM (0.00347) and WA (0.0031) groups was substantially higher than that for the CM (0.00256) and CA (0.00074) groups, which is consistent with the result of Watterson estimator analysis (θ_w-WM: 0.00256, θ_w-WA: 0.00218, θ_w-CM: 0.00151, and θ_w-CA: 0.00069). Furthermore, different groups exhibited different degrees of heterozygosity (Supplementary Fig. 5) and we also

observed gene-flow between these groups, which may be due to the overlapping distribution of accessions, open pollination and modern breeding program (Supplementary Fig. 6). The decay of linkage disequilibrium (LD) with physical distance between SNPs to half of the maximum values occurred at 22.0 kb and 20.6 kb in the WM (r^2 = 0.17) and WA (r^2 = 0.14) groups, respectively, which were considerably smaller than that in the CM (58.0 kb, r^2 = 0.31) and CA (610.2 kb, r^2 = 0.43) groups (Fig.1d). These results together are strongly suggestive of a significant genetic diversity reduction in cultivated melon because of domestication. Notably, the CA group has much lower nucleotide diversity and higher LD decay than the CM group, suggesting that the CA group has undergone a more severe bottleneck during domestication.

Independent domestication of *melo* and *agrestis* melon

Since the Neolithic revolution and the development of agriculture, human preferably kept and propagated seeds from wild plants with larger and more delicious fruits. To identify potential selective signals during melon domestication, we scanned genomic regions showing drastic reduction in nucleotide diversity by comparing each cultivated group with its corresponding wild group (π_{WM}/π_{CM} and π_{WA}/π_{CA}) over 50 kb windows. We identified 148 and 185 putative selection sweeps associated to domestication in *melo* ($\pi_{WM}/\pi_{CM} \geq$ 3.49) and *agrestis* ($\pi_{WA}/\pi_{CA} \geq$ 26.18), respectively, covering 6.28% (25.52 Mb) and 7.23% (29.39 Mb) of the assembled genome and harboring 1,481 and 1,710 genes (Supplementary Tables 5-8). Notably, only 143 of 27,427 genes (2.67 Mb; 0.66% of the assembled genome) were shared between the *melo* and *agrestis* sweeps (Supplementary Table 9). By contrast, in rice, most well-characterized domestication genes were shared between the *indica* and *japonica* types[27]. Jointly, the *melo* and *agrestis* sweeps cover 52.24 Mb (12.86% of the assembled genome), which encompasses 3,048 genes.

To discover potential domestication loci, we developed two F_2 segregating populations derived from a cross between a WM (MS-542) and a CM (additional accession B460), and a cross between a WA (additional accession yesheng) and a CA (MS-79), and identified 19 new QTLs that overlap with sweep regions, including 10 in *melo* and 9 in *agrestis* (Fig. 2a,b and Supplementary Table 10). Among the QTLs, one genomic region (~2.95-4.77 Mb on chromosome 8) related to fruit mass (*fwqaz8.1*, *fdqaz8.1*, *ftqaz8.1* for fruit weight, fruit diameter and flesh thickness, respectively) (Fig. 2c), a trait that has been under human selection was detected using the above F_2 segregating population from a cross between a WA and a CA accession. This region is consistent with a previously reported QTL (*fwqc8.1*) that contributes negatively to the increase of fruit weight in melon[28]. The nucleotide diversity of this interval was drastically reduced in the CA group compared to WA ($\pi_{WA}/\pi_{CA} = 7.45$), but the reduction was only minor in this region in CM ($\pi_{WM}/\pi_{CM} = 1.45$) (Fig. 2d). This region included two genes, *MELO3C007596* and *MELO3C007597*, both encoding auxin-responsive GH3-like proteins. Auxin-responsive GH3-like proteins are reported to be involved in fruit growth and development in longan[29] and tomato[30], suggesting both of the two genes are logical candidates to be associated with fruit mass during *agrestis* domestication. Moreover, we found that *Cm-HMGR* (*MELO3C026512*) on chromosome 3, which encodes a hydroxy-methylglutaryl coenzyme A reductase (HMGR) in the mevalonate (MVA) pathway that is involved in controlling fruit size in melon[31], was located in a *melo* domestication sweep ($\pi_{WM}/\pi_{CM} = 4.07$) (Fig. 2e).

Bitterness is an essential domestication trait, and has been (partially) lost during the domestication of melon. We observed that 95.18% of CM accessions carried non-bitter young fruits, whereas 25.87% of young fruits from the CA accessions were bitter, especially the fruits exposed to stress conditions. This suggests that the two melon groups

possess different domestication mechanisms conferring the loss of bitterness. We detected a notable decrease in nucleotide diversity in the *Bi* (encoding a cucurbitadienol synthase) cluster (π_{WM}/π_{CM} = 3.61 and π_{WA}/π_{CA} = 1.75) in *melo* and in the *CmBt* locus (encoding a transcription factor that activates *CmBi* transcription)[32] in *agrestis* (π_{WA}/π_{CA} = 28.21 and π_{WM}/π_{CM} = 3.70) (Fig. 2a,b). Additionally, there is an obvious population differentiation in *CmBi* and *CmBt* between the CM and CA groups (Fig. 2f,g).

To further verify potential sweeps related to bitterness during melon domestication, we performed QTL mapping using the above two F_2 populations (WM × CM and WA × CA). Two QTLs (~29.04-29.93 and ~21.07-22.05 Mb on chromosome 11 and 9, respectively) associated with fruit bitterness were identified in *melo* and *agrestis*, harboring the *CmBi*[32] and the *CmBt* gene[32], respectively (Fig. 2f,g). In general, alleles from different bitterness-related genes have been domesticated in the two melon subspecies. This was further validated by assessment of gene expression (Fig. 2h,i and Supplementary Fig. 7) and cucurbitacin B content (Supplementary Table 11). Furthermore, we found that hybrids (F_1) from a cross between non-bitter CM (accession MS-251) and CA (accession MS-42) lines always had bitter young fruits, suggesting that complementary genes exist conferring bitterness, as previously hypothesized[33,34].

Acidity as one major component of taste is selected by farmers and breeders during melon breeding. The acidic genotype is presumably the ancestral form[35], and the acidity in domesticated *melo* and *agrestis* too seems to be related to different genes. For example, we found that one domestication sweep (π_{WA}/π_{CA} = 1.94 and π_{WM}/π_{CM} = 9.99) containing the *CmPH* gene (*MELO3C025264*)[35] on chromosome 8 occurred in the *melo* but not in the *agrestis* group (Fig. 2a,b). The *CmPH* gene, encoding a transmembrane transporter, determines fruit acidity based on the presence of an insertion of a four amino-acid

duplication in non-acidic melon accessions, and contributes to the evolution of sweet melons[35]. We further verified the causative variation and found that the insertion occurred in non-acidic melon accessions of the CM group, but not all accessions were consistent in the CA group, suggesting that other genes might contribute to the acidity in the CA group. The *CmPH* gene was also detected within the association signals in a GWAS analysis for flesh acidity in *melo* accessions (Fig. 2j), and located in a *melo* sweep (Fig. 2a). Intriguingly, *MELO3C011482* on chromosome 3 encoding a ATP-citrate synthase subunit 1 was located in an association signal (Fig. 2k) and a sweep of *agrestis* (Fig. 2b).

In summary, our results suggest that distinct domestication mechanisms for fruit mass, flesh bitterness and acidity occurred in *melo* and *agrestis* accessions, which further supports the hypothesis that the CM and CA groups were domesticated independently from the WM and WA groups, respectively.

Divergence between the *melo* and *agrestis* groups

Melon is a diverse species cultivated by local farmers and used by breeders in many countries. Geographically, *melo* is cultivated worldwide, whereas *agrestis* is concentrated in East Asia. In general, cultivated *agrestis* melons possess greener leaves, edible epicarp, thinner flesh, lower sugar content and ecological differences resulting from their distinct geographical distributions. To dissect genomic regions underlying these differences, we measured the pairwise genome-wide fixation index (F_{ST}) values based on SNPs between different melon groups. The average F_{ST} value between the CM and CA groups was estimated at 0.46, which was similar to that of *indica* and *japonica* rice (0.55)[15], indicating strong population differentiation in the two subspecies. Based on F_{ST}, 289 divergent genomic regions between *melo* and *agrestis* were identified, which covered 56.9 Mb (14.01%) of the assembled genome and harboring 3,535 predicted genes (Supplementary

263 Tables 12 and 13).

264

265 Seventeen previously reported QTLs for flesh thickness and sugar content
266 overlapped with these divergent genomic regions (Supplementary Fig. 8a and
267 Supplementary Table 14). We also identified two new QTLs (Supplementary Fig. 8b,c)
268 for flesh thickness on chromosome 4 and 5 using an F_2 population from a cross between a
269 CM (additional accession Y14) and a CA line (MS-1006), both of which were close to
270 divergence regions. Intriguingly, one GWAS signal on chromosome 4 for ovary
271 pubescence, a trait used as to distinguish *melo* and *agrestis*[6], was also located in a
272 divergence region (Supplementary Fig. 8d). Furthermore, five xyloglucan
273 endo-transglycosylase genes involved in plant growth[36,37] were located in a divergence
274 region (~2.15-2.28 Mb) of chromosome 5. This dataset constitutes a relevant resource for
275 the exploitation of genes conferring genetic differentiation between *melo* and *agrestis*.

276

277 **Identification of genes or loci related to important agronomic traits**

278 Melon has several diverse characteristics of agronomic importance, such as sex
279 determination, peel and flesh color, and fruit shape. However, few genes or loci underlying
280 agronomic traits have been identified in melon so far. To explore the potential of GWAS to
281 identify causal genes for complex traits, we performed an association study using a panel
282 composed of 1,067 diverse accessions for 16 agronomic traits (Supplementary Table 15).
283 A total of 208 significant association signals were identified in the melon genome. Four
284 previously dissected genes were found in these association signals, including *CmACS-7*
285 for monoecy[12], *CmOr* for flesh color[13], *CmKFB* for peel color[14] and *CmPH* for acidity[35]
286 (Fig. 2 and Supplementary Fig. 9). The remaining 204 signals were associated with yield
287 (76), fruit quality (29) and morphological (99) traits (Supplementary Figs. 10-20). We
288 further validated major GWAS signals for rind sutures, peel color and flesh color using
289 segregating populations and molecular biology approaches (Fig. 3,4 and Supplementary

290 Fig. 21).

291

292 Rind sutures (also called vein tracks) is an important trait commonly found in
293 commercial melons, which is controlled by a single gene[38] on chromosome 11. A strong
294 GWAS signal for rind sutures was identified (P = 2.14 × 10^{-68}; ~20.6-24.8 Mb) on
295 chromosome 11 (Fig. 3a). To further validate this signal, we constructed a RIL population[39]
296 obtained by crossing a sutured line (MS-1152, Vedrantais) with a non-sutured line (Piel de
297 sapo T111) and narrowed down the QTL to a 1.7-Mb (~22.8-24.5 Mb) interval (Fig. 3b).
298 We further delimited this interval to an approximately 86-kb (~23.17-23.25 Mb) region
299 using additional F_2 and recombinant inbred line (RIL) populations. The region contains
300 four putative protein-encoding genes, of which two are expressed in flower and fruit
301 tissues (Fig. 3c). We found that *MELO3C019694*, encoding an AGAMOUS MADS-box
302 transcription factor, resides 16.8 kb upstream of the strongest association signal. The
303 orthologues of this gene include *SHP1* (*AT3G58780*) / *SHP2* (*AT2G42830*), which
304 regulate pod dehiscence in *Arabidopsis*[40], and *TAGL1* (*Solyc07g055920.2.1*), which is
305 required for pericarp expansion and climacteric ripening in tomato[41] (Fig. 3d).

306

307 We further analyzed the upstream and downstream sequences of *MELO3C019694* in
308 order to identify structural variations and discovered a 1,070-bp deletion at 23.85 kb
309 upstream of *MELO3C019694* that was present in most sutured accessions (83.66% of 257
310 accessions) (Fig. 3e,f). The expression level of *MELO3C019694* is delayed until seven
311 days after pollination in the sutured line compared to the non-sutured line, which is the
312 initial stage of suture development (Fig. 3g). These results indicate that *MELO3C019694*
313 could be a candidate gene for sutures, and the 1,070-bp deletion might impair the
314 transcriptional regulation of *MELO3C019694*. However, the mechanism and causal
315 variation of *MELO3C019694* need to be further validated functionally.

316

Peel and flesh color are important fruit quality traits influencing consumers' choice and acceptability. Peel colors of commercial melons are green, white or yellow (Fig. 4a), which are conferred by distinct pigment accumulation[42]. We identified a 12:3:1 segregation ratio for green, white and yellow traits by analyzing an F_2 segregating population from a cross between a green-peel (MS-723) and a yellow-peel (B432, an additional accession) lines (Fig. 4b), indicating that green peel is dominant epistatic to non-green (white and yellow) peel. We selected 254 green and 381 non-green accessions (145 white and 236 yellow accessions) in a GWAS analysis and identified two strong association signals on chromosome 4 ($-\log_{10}P$ value = 14.17) and chromosome 8 ($-\log_{10}P$ value =10.78) (Fig. 4c). Moreover, we performed a GWAS analysis using the non-green accessions (145 white and 236 yellow accessions). One significant peak ($-\log_{10}P$ value = 20.80) was detected on chromosome 10 (Fig. 4d).

To further verify these signals related to peel color, we sequenced three bulk populations with green, white and yellow peel from the above F_2 population (MS-723 × B432). We computed the differences of SNP indices (ΔSNP index)[43] between the green and non-green peel bulk populations, and between the white and yellow peel bulk populations, respectively, and identified a single overlapping genomic region with those of GWAS on chromosome 4 (Fig. 4c) and chromosome 10 (Fig. 4d), respectively. The overlapping genomic regions were also identified in another F_2 segregating population obtained by crossing a green peel line with a yellow peel line (Fig. 4e-g). Within these genomic intervals (~0.30-0.80 Mb on chromosome 4 and ~3.41-3.50 Mb on chromosome 10), we detected two candidate genes related to peel color, *MELO3C003375* on chromosome 4 encoding a two-component response regulator-like protein APRR2 and the already identified *CmKFB* gene on chromosome 10 negatively regulating naringenin chalcone accumulation[14]. The orthologous genes of *MELO3C003375* in cucumber (*w*)[44], watermelon (*ClCG09G012330*)[45], pepper (GeneBank No. KC175445)[46] and tomato

(*SolyC08g077230*)[46] have been demonstrated to control chlorophyll metabolism and pigment accumulation in fruit peel.

MELO3C003375 exhibited much higher transcript levels in green-peel lines than white and yellow-peel lines (Fig. 4h). There is hardly any expression of *CmKFB* in yellow-peel accession (Fig. 4i), consistent with its function of negatively regulating flavonoid accumulation. Additionally, we detected a gene (*MELO3C003097*) in the genomic interval (~29.74-29.77 Mb) of the association signal on chromosome 8, an ortholog of the Arabidopsis *SG1*, which encodes a Protein Slow Green 1, required for chloroplast development[47], and expressed in every peel color accessions (Fig. 4j). We speculate that *MELO3C003375* and *CmKFB* are associated with the green and yellow peel trait, respectively; *MELO3C003097* could be a minor gene involved in peel color formation.

Moreover, we performed GWAS on flesh color using 688 melon accessions. Besides the identified *Gf* gene (*CmOr*)[13] controlling orange flesh, we detected a strong association signal on chromosome 8 with a highest -log*P* value of 22.66 (Supplementary Fig. 21a). The association signal overlapped with the reported *Wf* locus[38] controlling white and green flesh. To identify the candidate gene, we constructed a RIL population[39] from a cross between an orange-flesh (MS-1152, Vedrantais) and a white-flesh (Piel de sapo T111) lines for QTL mapping, and detected a significant QTL (*LUMQU8.1*; ~29.63-29.87 Mb; LOD score = 10.23) corresponding to the *Wf* locus on chromosome 8 (Supplementary Fig. 21b). Combining the QTL with GWAS results, a 96-kb overlapping interval containing 11 protein-coding genes was detected (Supplementary Fig. 21c). A previously reported candidate gene *MELO3C003069* (ref. 48) for *Wf*, encoding a pentatricopeptide protein, is 202-kb away from our mapping interval. Among the 11 genes, we found that one gene, *MELO3C003097*, whose orthologue (*SG*1) in Arabidopsis was reported to be essential for

chloroplast development and chlorophyll biosynthesis[45]. The expression level of *MELO3C003097* during fruit development was significantly higher in green-flesh accession (MS-982) than in white-flesh accession (MS-531) (Supplementary Fig. 21d). These results suggest that *MELO3C003097* may be a strong candidate for the *Wf* locus. Interestingly, the same peak on chromosome 8 was found in GWAS for both peel and flesh color, indicating that this peak may play an important role in the color formation of both peel and flesh tissues in melon.

DISCUSSION

In summary, our analysis based on large-scale genome resequencing suggests three independent domestications of melon, one in Africa and two in India. Though the African clade (WAF and CAF) is clearly a different gene pool from *melo* (WM and CM) and *agrestis* (WA and CA) groups[5], there is a limited number of African accessions captured in our collection. Therefore, it would be worthwhile to explore a wider African diversity panel in future studies. The Indian domestication events were derived from distinct wild populations, and the small number of common selective sweeps suggests that domestication was achieved via diverse genetic pathways that ultimately resulted in similar phenotypes. The strong differentiation between *melo* and *agrestis* may be useful in breeding, because inter-subspecies crosses have the potential to generate heterosis and high diversity (Supplementary Note). Furthermore, our identification of candidate genes related to domestication and important agronomic traits (Supplementary Table 16) will be useful for melon breeding.

Acknowledgements We thank Dr. Brandon. S. Gaut (Department of Ecology and Evolutionary Biology, University of California Irvine, Irvine, CA, USA.), Dr. W. Lucas (University of California, Davis), Dr. J. Ruan (Agricultural Genome Institute at Shenzhen, Chinese Academy of Agricultural Sciences) and Dr. D. Wu (Kunming Institute of Zoology, Chinese Academy of Sciences) for critical comments. This work was supported by funding from the Agricultural Science and Technology Innovation Program (to Yongyang. Xu, S.H., Z.Z. and H.W.), the China Agriculture Research System (CARS-25 to Yongyang. Xu and H.W.), the Leading Talents of Guangdong Province Program (00201515 to S.H.), the Shenzhen Municipal (The Peacock Plan KQTD2016113010482651 to S.H.), the Dapeng district government, National Natural Science Foundation of China (31772304 to Z.Z.), the Science and Technology Program of Guangdong (2018B020202007 to S.H.), the National Natural Science Foundation of China (31530066 to S.H.), the National Key R&D Program of China (2016YFD0101007 to S.H.), USDA National Institute of Food and Agriculture Specialty Crop Research Initiative (2015-51181-24285 to Z.F.), the European Research Council (ERC-SEXYPARTH to A.B.), the Spanish Ministry of Economy and Competitiveness (AGL2015–64625-C2-1-R to J.G.-M), Severo Ochoa Programme for Centres of Excellence in R&D 2016–2010 (SEV-2015–0533 to J.G.-M) and the CERCA Programme/Generalitat de Catalunya to J.G.-M, and the German Science Foundation (SPP1991 Taxon-OMICS to H.S.).

Author contributions S.H., Yongyang. Xu. and J.G.-M. designed studies and contributed to the original concept of the project, S.H., G.Z., T.L., Z.Z. and Q.F. managed the project, T.G., I.J., R.W., V.R. and W.F performed the bioinformatics, S.M., J.S., Yongyang. Xu., M. Pitrat., C.D., J.W., J.L. and A.J.M. contributed to the collection the melon accessions, Y.H., G.Z., W.K., H.W., J.Z., Z.X., A.G., N.K., E.O., D.S., S.Z., Y.Z. and N.L. planted accessions, prepared the samples and performed phenotyping, P.W., Y.H., Y.Z., J.A., C.M., L.P., M. Pujol. and D.O. designed and performed the molecular experiments, G.Z., Q.L. and T.L.

prepared the figures and tables, S.H., T.L., J.G.-M., Z.F., T.G., A.J.M., V.R., A.G., Yong. Xu., A.B., H.S. and J.J. revised the manuscript, G.Z., Q.L. T.L., Z.Z. and Q.F. analyzed whole data and wrote the paper.

Competing interests The authors declare no competing interests.

References

1 Pitrat, M., Hanelt, P. & Hammer, K. Some comments on infraspecific classification of melon. *Acta Horticulturae* **510**, 29-36 (2000).

2 Luan, F., Delannay, I. & Staub, J. E. Chinese melon (*Cucumis melo* L.) diversity analyses provide strategies for germplasm curation, genetic improvement, and evidentiary support of domestication patterns. *Euphytica* **164**, 445-461 (2008).

3 Kerje, T. & Grum, M. The origin of melon, *Cucumis melo*: a review of the literature. *Acta Horticulturae* **510**, 37-44 (2000).

4 Sebastian, P., Schaefer, H., Telford, I. R. & Renner, S. S. Cucumber (*Cucumis sativus*) and melon (*C. melo*) have numerous wild relatives in Asia and Australia, and the sister species of melon is from Australia. *Proc. Natl. Acad. Sci. USA* **107**, 14269-14273 (2010).

5 Endl, J. et al. Repeated domestication of melon (*Cucumis melo*) in Africa and Asia and a new close relative from India. *Am. J. Bot.* **105**, 1662-1671 (2018).

6 Jeffrey, C. A review of the Cucurbitaceae. *Botanical Journal of the Linnean Society* **81**, 233-247 (1980).

7 Serres-Giardi, L. & Dogimont, C. *How microsatellite diversity helps to understand the domestication*. in Proceedings of Xth EUCARPIA meeting on genetics and breeding of Cucurbitaceae (eds. Sari, N., Solmaz, I. & Aras, V.) 254-263 (Antalya, 2012).

8 Staub, J. E., Lopez-Sese, A. I. & Fanourakis, N. Diversity among melon landraces (*Cucumis melo* L.) from Greece and their genetic relationships with other melon germplasm of diverse origins. *Euphytica* **136**, 151-166 (2004).

9 Tanaka, K. et al. Seed size and chloroplast DNA of modern and ancient seeds explain the establishment of Japanese cultivated melon (*Cucumis melo* L.) by introduction and selection. *Genetic Resources and Crop Evolution* **63**, 1237-1254 (2015).

10 Paris, H. S., Amar, Z. & Lev, E. Medieval emergence of sweet melons, *Cucumis melo* (Cucurbitaceae). *Ann. Bot.* **110**, 23-33 (2012).

11 Garcia-Mas, J. et al. The genome of melon (*Cucumis melo* L.). *Proc. Natl. Acad. Sci. USA* **109**, 11872-11877 (2012).

12 Boualem, A. et al. A conserved mutation in an ethylene biosynthesis enzyme leads to andromonoecy in melons. *Science* **321**, 836-838 (2008).

13 Tzuri, G. et al. A 'golden' SNP in *CmOr* governs the fruit flesh color of melon (*Cucumis melo*). *Plant J.* **82**, 267-279 (2015).

14 Feder, A. et al. A kelch domain-containing F-Box coding gene negatively regulates flavonoid accumulation in muskmelon. *Plant Physiol.* **169**, 1714-1726 (2015).

15 Huang, X. et al. Genome-wide association studies of 14 agronomic traits in rice landraces. *Nat. Genet.* **42**, 961-967 (2010).

16 Tian, F. et al. Genome-wide association study of leaf architecture in the maize nested association mapping population. *Nat. Genet.* **43**, 159-162 (2011).

17 Jia, G. et al. A haplotype map of genomic variations and genome-wide association

studies of agronomic traits in foxtail millet (*Setaria italica*). *Nat. Genet.* **45**, 957-961 (2013).

18 Zhou, Z. et al. Resequencing 302 wild and cultivated accessions identifies genes related to domestication and improvement in soybean. *Nat. Biotechnol*. **33**, 408-414 (2015).

19 Du, X. et al. Resequencing of 243 diploid cotton accessions based on an updated A genome identifies the genetic basis of key agronomic traits. *Nat. Genet.* **50**, 796-802 (2018).

20 Shang, Y. et al. Biosynthesis, regulation, and domestication of bitterness in cucumber. *Science* **346**, 1084-1088 (2014).

21 Tieman, D. et al. A chemical genetic roadmap to improved tomato flavor. *Science* **355**, 391-394 (2017).

22 Zhu, G. et al. Rewiring of the fruit metabolome in tomato breeding. *Cell* **172**, 249-261 (2018).

23 Argyris, J. M. et al. Use of targeted SNP selection for an improved anchoring of the melon (*Cucumis melo* L.) scaffold genome assembly. *BMC Genomics* **16**, 4 (2015).

24 Qi, J. et al. A genomic variation map provides insights into the genetic basis of cucumber domestication and diversity. *Nat. Genet.* **45**, 1510-1515 (2013).

25 Dhillon, N. P. S. et al. Diversity among landraces of Indian snapmelon (*Cucumis melo* var. *momordica*). *Genetic Resources and Crop Evolution* **54**, 1267-1283 (2007).

26 Tajima, F. Evolutionary relationship of DNA sequences in finite populations. *Genetics* **105**, 437-460 (1983).

27 Huang, X. et al. A map of rice genome variation reveals the origin of cultivated rice. *Nature* **490**, 497-501 (2012).

28 Diaz, A. et al. Quantitative trait loci analysis of melon (*Cucumis melo* L.) domestication-related traits. *Theor. Appl. Genet*. **130**, 1837-1856 (2017).

29 Kuang, J. F. et al. Two *GH3* genes from longan are differentially regulated during fruit growth and development. *Gene* **485**, 1-6 (2011).

30 Lin, T. et al. Genomic analyses provide insights into the history of tomato breeding. *Nat. Genet.* **46**, 1220-1226 (2014).

31 Kato-Emori, S., Higashi, K., Hosoya, K., Kobayashi, T. & Ezura, H. Cloning and characterization of the gene encoding 3-hydroxy-3-methylglutaryl coenzyme A reductase in melon (*Cucumis melo* L. *reticulatus*). *Mol. Genet. Genomics* **265**, 135-142 (2001).

32 Zhou, Y. et al. Convergence and divergence of bitterness biosynthesis and regulation in Cucurbitaceae. *Nat. Plants* **2**, 16183 (2016).

33 Ma, D., Sun. L., Gao, S., Hu, R. & Liu, M. Studies on the genetic pattern of bitter taste in yong fruit of melon (*Cucumis melo* L.). *Acta Horticulturae Sinica* **23**, 255-258 (1996).

34 Fujishita, N., Furukawa, H. & Morii, S. Distribution of three genotypes for bitterness of F_1 immature fruit in *Cucumis melo*. *Jpn. J. Breed* **43** (Suppl. 2), 206 (1993).

35 Cohen, S. et al. The *PH* gene determines fruit acidity and contributes to the evolution of sweet melons. *Nat. Commun*. **5**, 4026 (2014).
36 Nardi, C. F. et al. Expression of *FaXTH1* and *FaXTH2* genes in strawberry fruit. Cloning of promoter regions and effect of plant growth regulators. *Scientia Horticulturae* **165**, 111-122 (2014).
37 Dogra, V., Sharma, R. &Yelam, S. Xyloglucan endo-transglycosylase/hydrolase (XET/H) gene is expressed during the seed germination in *Podophyllum hexandrum*: a high altitude Himalayan plant. *Planta* **244**, 505-515 (2016).
38 Perin, C. et al. A reference map of *Cucumis melo* based on two recombinant inbred line populations. *Theor. Appl. Genet.* **104**, 1017-1034 (2002).
39 Pereira, L. et al. QTL mapping of melon fruit quality traits using a high-density GBS-based genetic map. *BMC Plant Biol*. **18**, 324 (2018).
40 Liljegren, S. J. et al. *SHATTERPROOF* MADS-box genes control seed dispersal in *Arabidopsis*. *Nature* **404**, 766-770 (2000).
41 Vrebalov, J. et al. Fleshy fruit expansion and ripening are regulated by the tomato *SHATTERPROOF* gene *TAGL1*. *Plant Cell* **21**, 3041-3062 (2009).
42 Tadmor, Y. et al. Genetics of flavonoid, carotenoid, and chlorophyll pigments in melon fruit rinds. *J. Agric. Food Chem*. **58**, 10722-10728 (2010).
43 Abe, A. et al. Genome sequencing reveals agronomically important loci in rice using MutMap. *Nat. Biotechnol.* **30**, 174-178 (2012).
44 Liu, H. et al. Map-based cloning, identification and characterization of the *w* gene controlling white immature fruit color in cucumber (*Cucumis sativus* L.). *Theor. Appl. Genet*. **129**, 1247-1256 (2016).
45 Oren, E. et al. Multi-allelic *APRR2* gene is associated with fruit pigment accumulation in melon and watermelon. *J. Exp. Bot.* **70**, 3781–3794 (2019).
46 Pan, Y. et al. Network inference analysis identifies an *APRR2-like* gene linked to pigment accumulation in tomato and pepper fruits. *Plant Physiol*. **161**, 1476-1485 (2013).
47 Hu, Z. et al. The tetratricopeptide repeat-containing protein slow green1 is required for chloroplast development in *Arabidopsis*. *J. Exp. Bot.* **65**, 1111-1123 (2014).
48 Galpaz, N. et al. Deciphering genetic factors that determine melon fruit-quality traits using RNA-Seq-based high-resolution QTL and eQTL mapping. *Plant J.* **94**, 169-191 (2018).

Figure legends

Fig.1 Geographic distribution and population structure of melon accessions. **a**, Geographic distribution of melon accessions, which are represented by dots on the world map. **b**, Phylogenetic tree of the population (531 *C. melo* subsp. *melo*, 437 *C. melo* subsp. *agrestis* accessions and 9 wild relatives as the outgroup) constructed using 17,055 SNPs at four-fold degenerate sites. AF, African; WAF, wild African; CAF, cultivated African; WM, wild *melo*; CM, cultivated *melo*; WA, wild *agrestis*; CA, cultivated *agrestis*. Representative fruits of the three clades studied are shown. Scale bars represent 1.0 cm. **c**, Model-based clustering analysis with different numbers of clusters (K = 2, 3 and 4). The y axis quantifies clusters membership, and the x axis lists the different accessions. The orders and positions of these accessions on the x axis are consistent with those in the phylogenetic tree. **d**, Genome-wide average LD decay estimated from different melon group.

Fig. 2 Independent selection in domesticated traits between *C. melo.* subsp. *melo* and *agrestis*. **a,b**, Selection signals in domestication of *C. melo* subsp. *melo* (**a**) and *agrestis* (**b**) populations on the twelve melon chromosomes. Horizontal dashed lines indicate the genome-wide threshold of selection signals. Candidate genes previously reported or identified in this study (red) and QTLs (black) that overlapped with selective sweeps are marked. **c**, Overlapped genomic regions of QTLs for fruit weight, fruit diameter and flesh thickness mapped by genetic analysis of an F_2 population from the cross of a wild and a cultivated (MS-79) *agrestis* accession. **d,e**, Distribution of nucleotide diversity (π) of WA and CA (**d**), and WM and CM (**e**) accessions. *MELO3C007596*, *MELO3C007597* and *Cm-HMGR*[31] were located within the *agrestis* and *melo* sweep regions, respectively. **f,g**, QTL mapping for young fruit bitterness using two F_2 populations from the cross between wild *melo* (**f**) and *agrestis* (**g**) with their corresponding cultivated accessions. F_{ST} values of *CmBi*[32] and *CmBt*[32] genes between CM and CA are shown in the red vertical line. **h,i**, qRT-PCR of *CmBi* (**h**) and *CmBt* (**i**) in young fruits of cultivated *melo* and *agrestis* accessions. Data are presented as mean ± s.d. (n = 3 independent experiments).

j,**k**, Manhattan plots of GWAS for flesh acidity in *melo* (**j**) and *agrestis* (**k**) populations. *CmPH*[35] and *MELO3C011482* were identified residing within the association signals on chromosomes 8 and 3, respectively.

Fig. 3 Identification of a candidate gene for the melon sutures trait. **a**, Manhattan plots of GWAS for fruit sutures in melon accessions. Fruits of representative sutured and non-sutured melon accessions are shown. Scale bars represent 1.0 cm. **b**, Fine mapping of melon fruit sutures using diverse segregating populations. An 86-kb interval harboring four genes was identified (represented by arrows, of which the green one is the candidate gene *MELO3C019694*). **c**, Expression of the four genes in flower and developed fruit of different genotypes. **d**, Phylogenetic tree of *MELO3C019694* and its homologues in rice (green points), Arabidopsis (red points), tomato (blue points), pumpkin (light blue points) and melon (purple points). The closest homologues of *MELO3C019694* indicated in a shadow box include those from Arabidopsis (*AT3G58780, AT2G42830*)[40] and tomato (*Solyc07g055920.2.1*)[41] that have been reported associated with pod dehiscence and pericarp expansion, respectively. **e**, Identification of a 1.07-kb deletion upstream of the *MELO3C019694* gene in accessions with sutures compared with non-sutured accessions. **f**, Proportion of the 1.07-kb deletion (purple) existing in sutured and non-sutured melon accessions. **g**, qRT-PCR analysis of *MELO3C019694* in the female flowers and young fruits in PS (a non-sutured accession) and VED (a sutured accession). fl develop: flower in development; closed fl: flower before anthesis; 0 DAP, 3 DAP and 7 DAP represent fruits at 0, 3, 7 days after pollination. Data are presented as mean ± s.d. (n = 3 independent experiments).

Fig. 4 GWAS, BSA and QTL analyses identified the same region as being potentially important for peel color. **a**, Phenotypes of green, white and yellow-peel melon accessions. Scale bars represent 1.0 cm. **b**, Segregation of peel color in an F_2 population derived from crossing a green-peel accession (MS-723) with a yellow-peel accession (B432). **c,d,** Identification of overlapping intervals using GWAS and BSA analyses for the peel color trait in melon. GWAS analyses (Manhattan plots) were performed using green, white and yellow-peel melon accessions (**c**), and white and yellow-peel melon accessions (**d**), respectively. BSA analyses (red lines) were conducted with the green and non-green (white and yellow) bulks (**c**), and the white and yellow bulks (**d**) from the above F_2 population. Candidate gene in each signal is provided. The horizontal dashed lines indicate the genome-wide threshold of GWAS signals (*P*-value = 2.51×10^{-6}). **e-g,** QTL mapping using another F_2 population derived from crossing a green-peel accession and a yellow-peel accession. Candidate genes (in green), *MELO3C003375* and *CmKFB*[14], were located in the intervals of the identified QTLs. **h-j**, qRT-PCR analysis of *MELO3C003375*, *CmKFB*[14] and *MELO3C003097* during fruit development in melon accessions with different peel colors. Data are presented as mean ± s.d. (n = 3 independent experiments)

Materials and Methods

Plant materials and sequencing

A diverse worldwide collection of 1,175 melon accessions and 9 from related species of the *Cucumis* genus was obtained from NMGWM (National Mid-term Genebank for Watermelon and Melon, Zhengzhou, China), ZFRI-CAAS (Zhengzhou Fruit Research Institute, Chinese Academy of Agricultural Sciences), USDA (US Department of Agriculture) and INRA (National Institute for Agricultural Research). Information about the accessions, including individual name, country of origin, group, varieties identity and resequencing data summary, is provided in Supplementary Table 1. Genomic DNA was extracted from fresh young leaves using the cetyltriethylammnonium bromide (CTAB) method[49]. At least 5 μg of genomic DNA was used for each accession to construct sequencing libraries according to the manufacturer's instructions (Illumina Inc). The libraries were sequenced on the Illumina HiSeq 2500 or HiSeq 3000 platform, generating 150-bp or 125-bp paired-end reads. Five F_2 populations were used in our study, of which the genome of individuals of three F_2 populations were sequenced with 5 × depth, three bulks developed from an F_2 population were sequenced with 15 × depth.

Sequence alignment and variation calling

To call SNPs, reads of all accessions were mapped to the melon reference genome[23] (version 3.5.1) using SOAP2 (ref. [50]) with the following parameters: -m 100 -x 888 -s 35 -l 32 -v 3. Mapped reads were filtered to remove PCR duplicates, assigned to chromosomes and sorted according to the mapping coordinates. Both pair-end and single-end mapped reads were used for SNP detection throughout the entire collection of melon accessions.

We identified possible SNPs for each accession relative to the reference using SOAPsnp[51] with the following parameters: -L 150 -u -F 1. The likelihood of each individual's genotype in glf format was then generated for each chromosome with SNP quality ≥ 40 and base quality ≥ 40.

To integrate SNPs across the entire collection, we called each SNP using GLFmulti[52] according to the maximum-likelihood estimation of site frequency. The core set of SNPs was obtained by filtering on the base of allele frequency and the quality score given by GLFmulti[52]. SNPs were further filtered using the following criteria: (i) one position with more than two alleles was considered to be a polymorphic site in the population and was excluded in the next analyses; (ii) the total sequencing depth should be > 500 × and < 6,800 × and the SNP quality value should be greater than 40; (iii) position with an average mapping rate of reads of less than 1.5 were retained to rule out the effect of duplications; and (iv) the nearest SNPs should be more than 1 bp away.

To obtain the final set of SNPs, we further performed filtering using segregation tests,

which can distinguish any segregation pattern from random sequencing errors on the base of the sequencing depth of the two putative alleles in different individuals. Permutations were used to determine the significance of allele depth in the population, and only sites with $P < 0.01$ were retained. To detect small indels (≤ 5 bp in length), we mapped all the sequence reads from each accession with a gap of ≤ 5 bp allowed (parameter -g 5) using SOAP2 (ref. [50]). Indels (1-5 bp) were called by SOAPindel pipeline.

Planting and phenotyping

A total of 1175 melon accessions and 9 from related species were grown in Zhengzhou (Henan province), Sanya (Hainan province) and Changji (Xinjiang province) in 2015 and 2016. Because of poor adaptation for some accessions, several traits were evaluated in only one or two locations. Three replicates were performed at each location.

Three RIL populations[39,53,54] and five F_2 populations were used to identify candidates for sutures, peel color, flesh color, fruit bitterness, flesh thickness and sugar content (Supplementary Table 17). We phenotyped for traits of fruit suture (as a qualitative trait for presence/absence) or flesh color as a qualitative trait for yellow, green or white at harvest. For flesh color, ripe fruit was cut in two longitudinal sections, and one of them was used to evaluate flesh color visually and scanned to perform the flesh color analysis in color spaces RGB and CIElab using the Tomato Analyzer 3.0 software[55,56]. Total chlorophyll and carotenoid contents were determined using UV-VIS Spectroscopy. The other accessions and populations were grown in Xinxiang, Sanya or Beijing and phenotyped following a Chinese technical specification for evaluating melon[57].

Phylogenetic and population structure analyses

A subset of 17,055 SNPs with a minor allele frequency (MAF) ≥ 0.05 and missing rate ≤ 0.4 at four-fold degenerate sites representing neutral or near-neutral variants, were used for phylogenetic and population structure analyses. The alignment was trimmed using trimAl[58] (version 1.4. rev22v) in order to remove positions that are non-variable and include more than 90% of gaps. The remaining sites were employed to construct the phylogenetic tree with RAxML[59] (version 8.1.17) using the evolutionary model GTR. The branch length and rate parameters were optimized, and the aLRT SH-like branch support was calculated using PhyML v3.0 (ref. [60]) with the options '-b -4, -o lr'. The same method was used to construct the phylogenetic tree of chloroplast genome. Population structure was investigated using the program STRUCTURE[61] (version 2.3.1), with the same data used in the phylogenetic tree construction. Furthermore, to confirm the result of STRUCTURE, we also perforemed the analysis using DAPC in R package *adegenet* 2.1.0 (ref. [62]) with the parameter "max.n.clust = 40, PCs to retain = 900, discriminant functions to retain = 5". In addition, principal component analysis (PCA) using the whole-genome SNPs with missing value ≤ 40% was performed with the EIGENSOFT 6.0.1 (ref. [63]). Combining with the phylogenetic tree and principal

component analyses, we classified these accessions into three distinct clades (African group, *melo* group and *agrestis* group). Considering the passport information, the *melo* group and *agrestis* groups could be further divided into two sub-clades (wild *agrestis*, cultivated *agrestis*; wild *melo* and cultivated *melo* groups), respectively.

Identification of domestication sweeps

To detect genomic regions affected by domestication, we measured the level of genetic diversity (π) using a 50-kb window with a step size of 5 kb in WM, CM, WA and CA, respectively. Genome regions affected by domestication should have substantially lower diversity in CM (π_{WM}) and CA (π_{WA}) than that in WM (π_{WM}) and WA (π_{WA}), respectively. Windows with π_{WM} or π_{WA} lower than 0.002 were excluded from the analysis. Windows with the top 5% highest ratios of π_{WM}/π_{CM} (≥ 3.49) or π_{WA}/π_{CA} (≥ 26.18) were selected as candidate domestication sweeps. We also performed QTL mapping for fruit mass and bitterness to analyze QTLs or genes that segregated between the wild and cultivated parents by resequencing the individuals of two F_2 segregating populations derived from crossing between the wild and cultivated accessions. If genetic intervals of these QTLs and reported genes (loci) were close to or located in domestication sweeps, we considered them to be candidate domesticated QTLs or genes (Supplementary Table 10).

Identification of differentiated regions

The population fixation statistics (F_{ST}) were estimated for 50-kb sliding windows with a step size of 5 kb and for each SNP using a variance component approach implemented in the HIERFSTAT R package[64]. The average F_{ST} of all sliding windows was regarded as the value at the whole-genome level across different groups. Sliding windows with the top 10% highest F_{ST} values were selected initially. Neighboring windows were then merged into one fragment. If the distance between two fragments was < 50 kb, fragments were merged into one region. The final merged regions were considered as highly diverged between different groups.

Watterson estimator analysis

The Watterson estimator of θ_w was evaluated using the software VariScan 2.0.3 (ref. [65]) for four main sub-populations. SNPs with a minor allele frequency (MAF) $\geq$ 1% within each sub-population were used as the input data. A sliding window of 50 kb in length was used to scan the whole genome. The average θ_w value of all windows in the genome was then calculated to present the polymorphism.

Linkage disequilibrium analysis

Haploview software[66] was used to calculate LD values for each of the groups (WM, CM, WA, CA) using SNPs with MAF $\geq$ 0.05 with the following parameters: -n -pedfile -info -log -maxdistance 1000 -minMAF 0.05 -hwcutoff 0 -dprime -memory 10480. LD decay was measured on the basis of the r^2 value and the corresponding distance between two

given SNPs.

HPLC analysis of cucurbitacin B

Fruit flesh and leaf samples were frozen in liquid nitrogen and ground in a mortar and pestle. The fine powder (0.5 g) was added to methanol (2 mL) and homogenized for 15 min, followed by centrifugation at 10,000 g at 4 °C for 10 min. The solution was filtered through 0.22 μm membrane prior to injection and then analyzed on an HPLC system (Agilent 1200) equipped with an XDB-C18 column (5 μm, 150 × 4.6 mm) and eluted with 55% methanol at 1 mL/min under a wavelength of 230 nm.

Genome-wide association studies

Only SNPs with minor allele frequency ≥ 0.05 and missing rate ≤ 0.4 in a population were used to carry out GWAS. This resulted in 1,599,428, 872,244 and 2,028,259 SNPs that were used in GWAS for subspecies of *melo*, *agrestis* and the entire population (*melo* and *agrestis*), respectively. We performed GWAS using Efficient Mixed-Model Association eXpedited (EMMAX) program[67]. Population stratification and hidden relatedness were modeled with a kinship (*K*) matrix in the emmax-kin-intel package of EMMAX. The *P*-value thresholds for significance were approximately 2.51×10^{-6}.

Bulked segregant analysis of F_2 population by whole-genome resequencing

We planted 450 individuals of an F_2 population derived from a cross between MS-723 (green-peel accession) and B432 (yellow-peel accession) in the winter of 2017 in Sanya, China. The fruit peel color of each individual was recorded. Genomic DNA was isolated from fresh leaves using the CTAB method. For bulked segregant analysis, bulked DNA samples were constructed by mixing equal amounts of DNA from 30, 29 and 9 individuals showing representative green, white and yellow peel color, respectively. Roughly 13 × genome sequences for each of the two parents (B432 and MS-723) and 15 × data for each of the three bulked samples (green peel, white peel and yellow peel) were generated. Short reads were aligned against the reference genome[23] (released 3.5.1) using the Burrows-Wheeler Aligner (BWA)[68], and SNPs were identified using SAMtools[69]. The average SNP index for the green-peel bulk and non-green-peel bulk (white-peel bulk and yellow-peel bulk), and white-peel bulk and yellow-peel bulk were calculated using a 1,000-kb sliding window with a step size of 100 kb.

Expression analysis of candidate genes for peel color, flesh color and suture

Fruits of MS-348 (yellow peel, orange flesh), MS-531 (white peel, white flesh) and MS-982 (green peel, green flesh) were sampled at 20, 25, 30, 35 and 40 days after pollination, respectively. Total RNA was extracted using RNAprep Pure plant kit (TIANGEN Biotech). The first-strand cDNA synthesis was conducted following SuperScript RT Mix (Bio-Connect Biotech). Then 2-μl cDNA was used to preform qRT-PCR in a 10-μl reaction mixture. We conducted the expression of *MELO3C003375*,

CmKFB and *MELO3C003097* in the peel of MS-348, MS-531 and MS-982, and the expression of *MELO3C003097* in flesh of MS-982 and MS-531. Expression of *CmBi* and *CmBt* were performed in fruits at 7 days after anthesis of cultivated *melo* and *agrestis* accessions. For suture, we harvested MS-1152 (sutured line) and Piel de sapo T111 (non-sutured line) at Fl-develop (7 mm-female flower), closed-Fl (10 mm-female flower) and 0, 3, 7 days after pollination, respectively, and calculated the expression of the candidate *MELO3C019694*. Three replicates were performed for each experiment. Relative expression levels were calculated by the $2^{-\Delta\Delta Ct}$ or $2^{-\Delta Ct}$ method.

Reporting Summary.

Further information on research design is available in the Nature Research Reporting Summary linked to this article.

Statistical analysis

Chi-square test statistic and standard deviation (stdev) were performed with the SPSS software. The significance was determined by two-tailed Student's t tests.

Code availability

All codes are available from the corresponding author upon request.

Data Availability

The raw sequence data reported in this paper has been deposited in the Sequence Read Archive (SRA) under accession PRJNA565104 that are publicly accessible.

References

49 Gawel, N. J. & Jarret, R. L. A modified CTAB DNA extraction procedure for *Musa* and *Ipomoea*. *Plant molecular biology* **9**, 262-266 (1991).

50 Li, R. et al. SOAP2: an improved ultrafast tool for short read alignment. *Bioinformatics* **25**, 1966-1967 (2009).

51 Li, R. et al. SNP detection for massively parallel whole-genome resequencing. *Genome Res.***19**, 1124-1132 (2009).

52 He, W. et al. ReSeqTools: an integrated toolkit for large-scale next-generation sequencing based resequencing analysis. *Genet. Mol. Res.* **12**, 6275-6283 (2013).

53 Harel-Beja, R. et al. A genetic map of melon highly enriched with fruit quality QTLs and EST markers, including sugar and carotenoid metabolism genes. *Theor. Appl. Genet.* **121**, 511-533 (2010).

54 Gur, A. et al. Genome-wide linkage-disequilibrium mapping to the candidate gene level in melon (*Cucumis melo*). *Sci. Rep.* **7**, 9770 (2017)

55 Brewer, M. T. et al. Development of a controlled vocabulary and software application to analyze fruit shape variation in tomato and other plant species. *Plant Physiol.* **141**, 15-25 (2006).

56 Darrigues, A., Hall, J., Knaap, E. & Francis, D. M. Tomato analyzer-color test: a new tool for efficient digital phenotyping. *J. Amer. Soc. Hort. Sci.* **133**, 579-586 (2008).

57 Ma, S. et al. *Descriptors and data standard for melon* (*Cucumis melo* L.) (China Agriculture press, Beijing, 2006).

58 Capella-Gutierrez, S., Silla-Martinez, J. M. & Gabaldon, T. TrimAl: a tool for automated alignment trimming in large-scale phylogenetic analyses. *Bioinformatics* **25**, 1972-1973 (2009).

59 Stamatakis, A. RAxML version 8: a tool for phylogenetic analysis and post-analysis of large phylogenies. *Bioinformatics* **30**, 1312-1313 (2014).

60 Guindon, S. et al. New algorithms and methods to estimate maximum-likelihood phylogenies: assessing the performance of PhyML 3.0. *Syst. Biol.* **59**, 307-321 (2010).

61 Falush, D., Stephens, M. & Pritchard, J. K. Inference of population structure using multilocus genotype data: linked loci and correlated allele frequencies. *Genetics* **164**, 1567-1587 (2003).

62 Jombart, T. adegenet: a R package for the multivariate analysis of genetic markers. *Bioinformatics* **24**, 1403-1405 (2008).

63 Patterson, N., Price, A. L. & Reich, D. Population structure and eigenanalysis. *PLoS Genet.* **2**, e190 (2006).

63 Goudet J. Hierfstat, a package for R to compute and test hierarchical *F*-statistics. *Molecular Ecology Notes* **5**, 184-186 (2005).

64 Barrett, J. C., Fry, B., Maller, J. & Daly, M. J. Haploview: analysis and visualization of LD and haplotype maps. *Bioinformatics* **21**, 263-265 (2005).

65 Hutter, S., Vilella, A. J. & Rozas, J. Genome-wide DNA polymorphism analysesusing VariScan**.** *BMC Bioinformatics* 7**,** 409 (2006).

66 Barrett, J. C., Fry, B., Maller, J. & Daly, M. J. Haploview: analysis and visualization of LD and haplotype maps. *Bioinformatics* **21**, 263-265 (2005).
67 Kang, H. M. et al. Variance component model to account for sample structure in genome-wide association studies. *Nat. Genet.* **42**, 348-354 (2010).
68 Li, H. & Durbin, R. Fast and accurate short read alignment with Burrows-Wheeler transform. *Bioinformatics* **25**, 1754-1760 (2009).
69 Li, H. et al. The Sequence Alignment/Map format and SAMtools. Bioinformatics 25, 2078-2079 (2009)

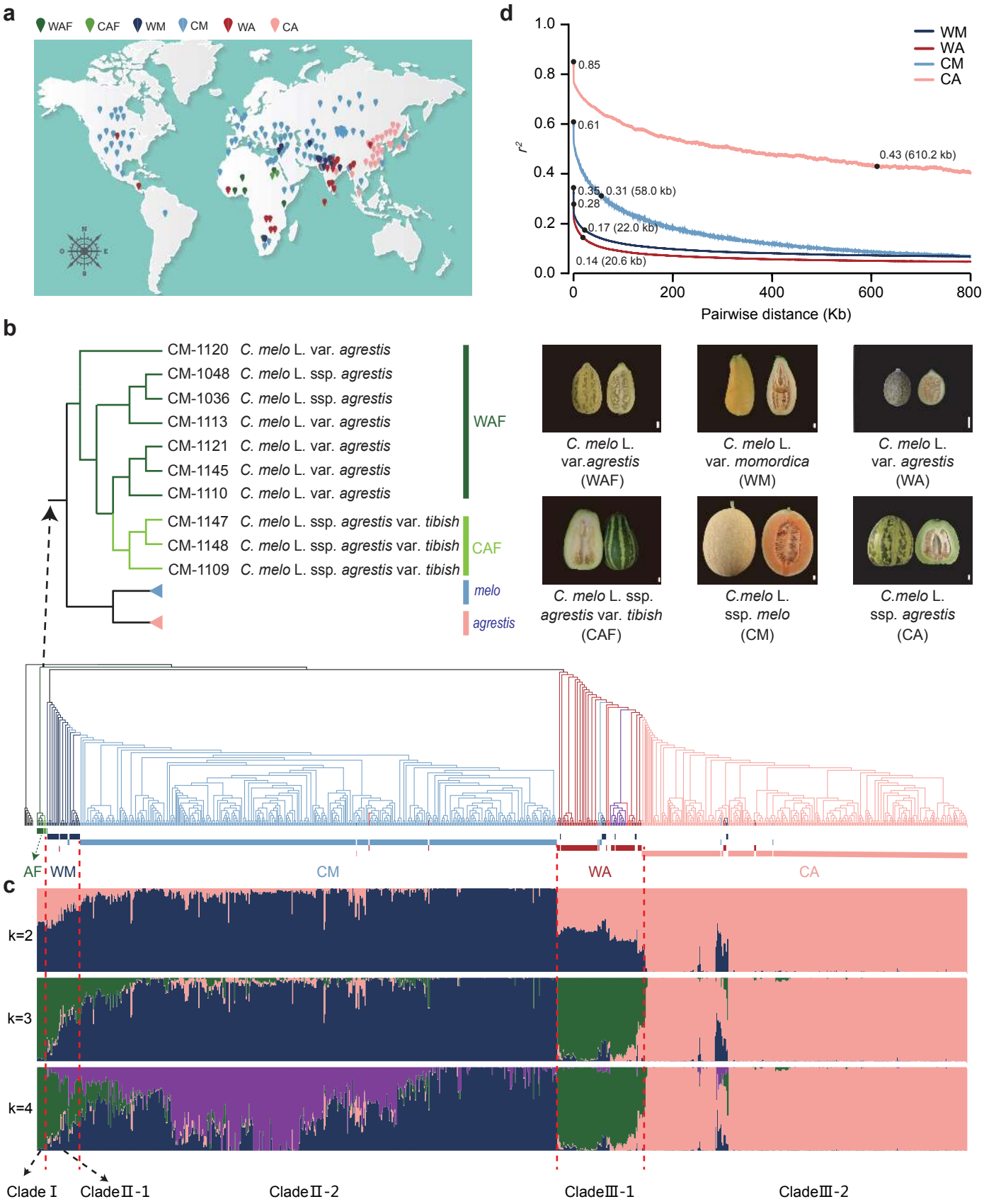
a
WAF
CAF
WM
CM
WA
CA
d
WM
WA
CM
CA
1.0
0.8
0.6
0.4
0.2
0.0
r^2
0.85
0.61
0.43 (610.2 kb)
0.35
0.31 (58.0 kb)
0.28
0.17 (22.0 kb)
0.14 (20.6 kb)
0
200
400
600
800
Pairwise distance (Kb)
b
CM-1120 C. melo L. var. agrestis
CM-1048 C. melo L. ssp. agrestis
CM-1036 C. melo L. ssp. agrestis
CM-1113 C. melo L. var. agrestis
CM-1121 C. melo L. var. agrestis
CM-1145 C. melo L. var. agrestis
CM-1110 C. melo L. var. agrestis
CM-1147 C. melo L. ssp. agrestis var. tibish
CM-1148 C. melo L. ssp. agrestis var. tibish
CM-1109 C. melo L. ssp. agrestis var. tibish
WAF
CAF
melo
agrestis
C. melo L. var.agrestis (WAF)
C. melo L. var. momordica (WM)
C. melo L. var. agrestis (WA)
C. melo L. ssp. agrestis var. tibish (CAF)
C.melo L. ssp. melo (CM)
C.melo L. ssp. agrestis (CA)
AF
WM
CM
WA
CA
c
k=2
k=3
k=4
Clade Ⅰ
CladeⅡ-1
CladeⅡ-2
CladeⅢ-1
CladeⅢ-2

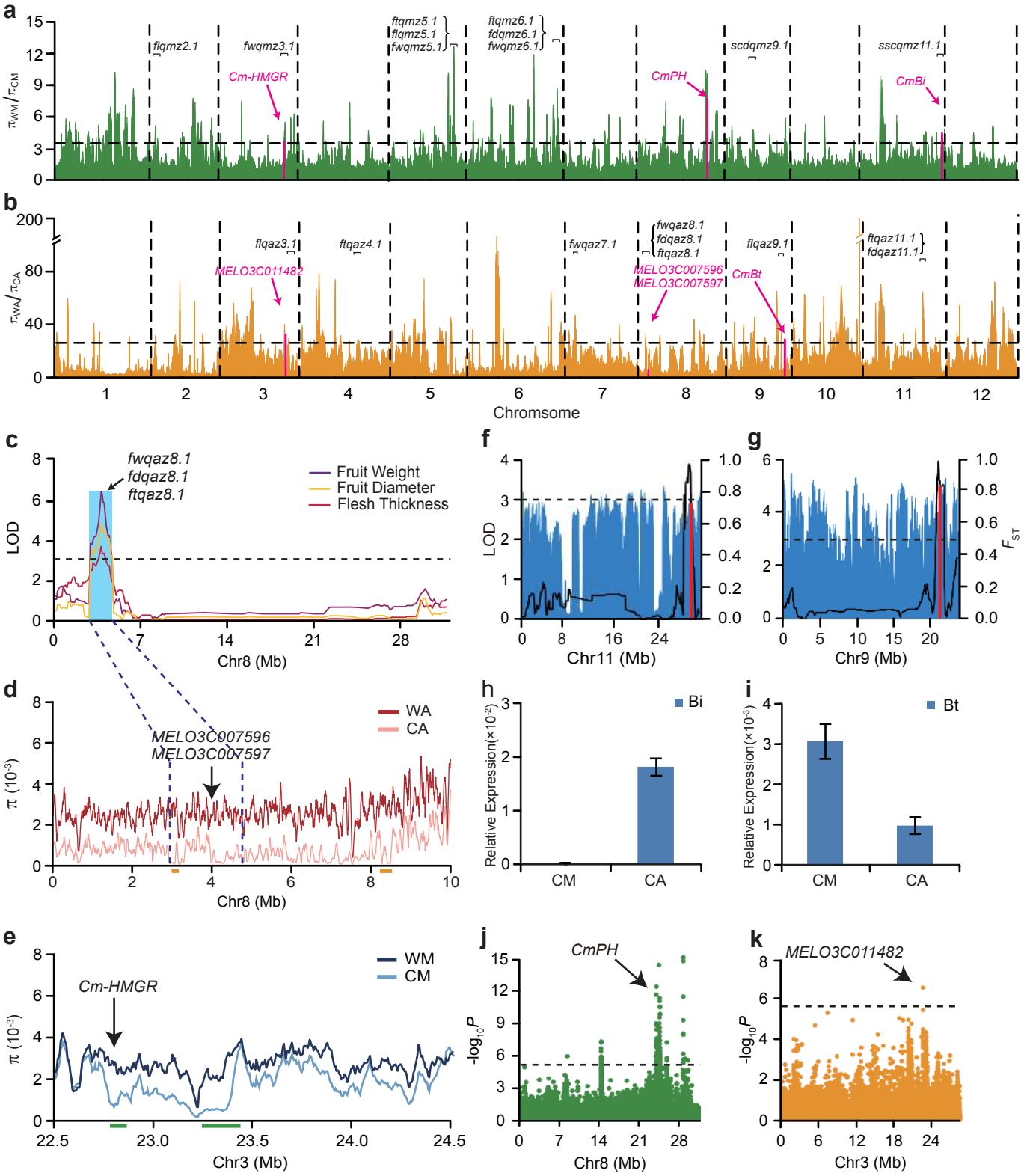
a
b
c
d
e
f
g
h
i
j
k
flqmz2.1
fwqmz3.1
Cm-HMGR
ftqmz5.1
flqmz5.1
fwqmz5.1
ftqmz6.1
fdqmz6.1
fwqmz6.1
CmPH
scdqmz9.1
sscqmz11.1
CmBi
flqaz3.1
MELO3C011482
ftqaz4.1
fwqaz7.1
fwqaz8.1
fdqaz8.1
ftqaz8.1
MELO3C007596
MELO3C007597
CmBt
flqaz9.1
ftqaz11.1
fdqaz11.1
Chromsome
Fruit Weight
Fruit Diameter
Flesh Thickness
Chr8 (Mb)
WA
CA
WM
CM
Chr3 (Mb)
Chr11 (Mb)
Chr9 (Mb)
Bi
Bt
Relative Expression
CM
CA

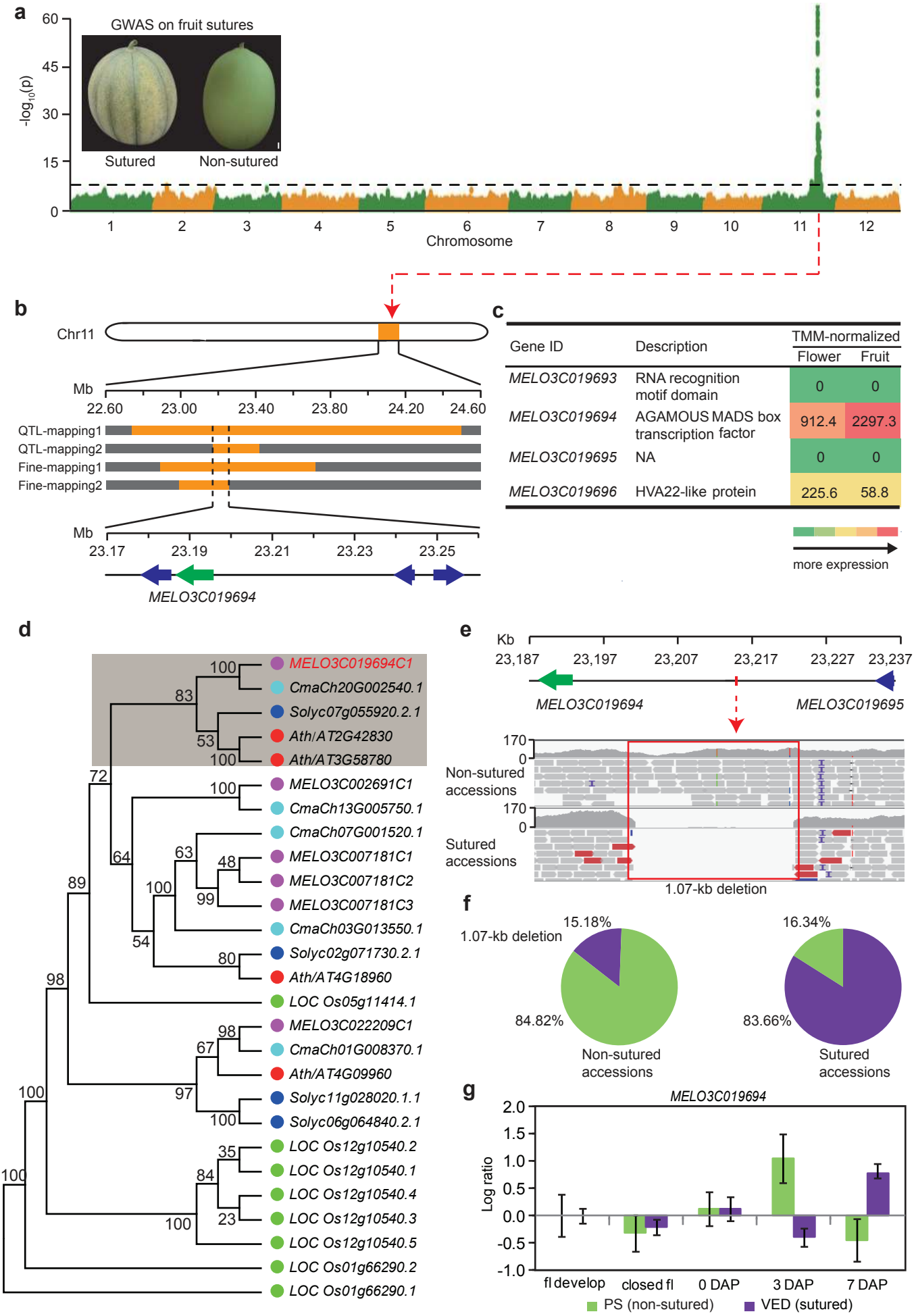
a
GWAS on fruit sutures
Sutured
Non-sutured
-log10(p)
Chromosome
b
Chr11
Mb
QTL-mapping1
QTL-mapping2
Fine-mapping1
Fine-mapping2
MELO3C019694
c
Gene ID
Description
TMM-normalized
Flower
Fruit
MELO3C019693
RNA recognition motif domain
MELO3C019694
AGAMOUS MADS box transcription factor
912.4
2297.3
MELO3C019695
NA
MELO3C019696
HVA22-like protein
225.6
58.8
more expression
d
MELO3C019694C1
CmaCh20G002540.1
Solyc07g055920.2.1
Ath/AT2G42830
Ath/AT3G58780
MELO3C002691C1
CmaCh13G005750.1
CmaCh07G001520.1
MELO3C007181C1
MELO3C007181C2
MELO3C007181C3
CmaCh03G013550.1
Solyc02g071730.2.1
Ath/AT4G18960
LOC Os05g11414.1
MELO3C022209C1
CmaCh01G008370.1
Ath/AT4G09960
Solyc11g028020.1.1
Solyc06g064840.2.1
LOC Os12g10540.2
LOC Os12g10540.1
LOC Os12g10540.4
LOC Os12g10540.3
LOC Os12g10540.5
LOC Os01g66290.2
LOC Os01g66290.1
e
Kb
MELO3C019694
MELO3C019695
Non-sutured accessions
Sutured accessions
1.07-kb deletion
f
1.07-kb deletion
15.18%
84.82%
Non-sutured accessions
16.34%
83.66%
Sutured accessions
g
MELO3C019694
Log ratio
fl develop
closed fl
0 DAP
3 DAP
7 DAP
PS (non-sutured)
VED (sutured)

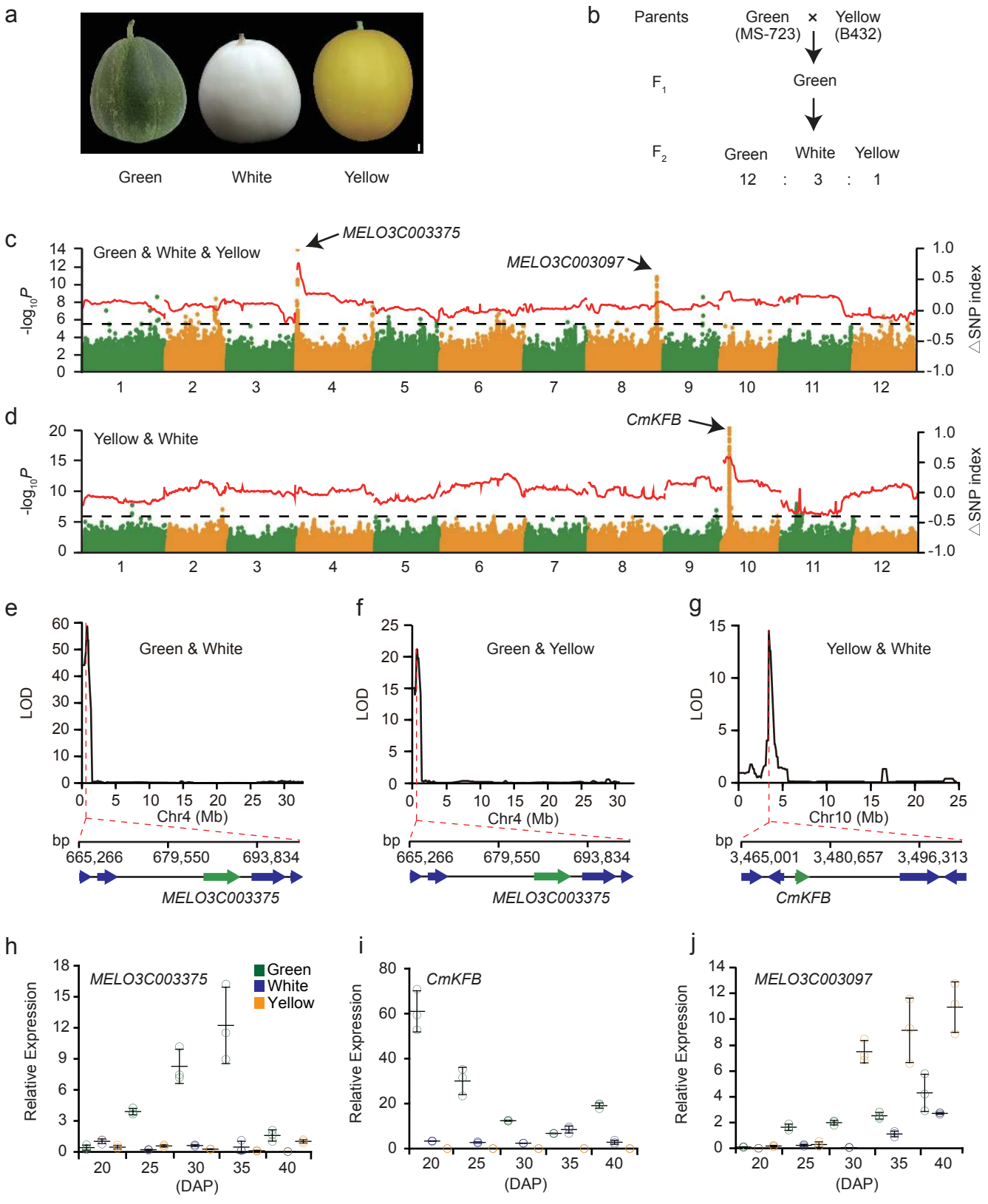
a
Green
White
Yellow
b
Parents
Green (MS-723) × Yellow (B432)
F1
Green
F2
Green White Yellow
12 : 3 : 1
c
Green & White & Yellow
MELO3C003375
MELO3C003097
-log10P
△SNP index
d
Yellow & White
CmKFB
e
Green & White
LOD
Chr4 (Mb)
bp
665,266 679,550 693,834
MELO3C003375
f
Green & Yellow
g
Yellow & White
Chr10 (Mb)
3,465,001 3,480,657 3,496,313
CmKFB
h
MELO3C003375
Green
White
Yellow
Relative Expression
(DAP)
i
CmKFB
j
MELO3C003097